Journal of Materials and Engineering Structures

Research Paper

Coefficient of surface water absorption: A non-destructive test index for evaluation and quality grading of cover-concrete

Raphael Nnodim Uwazuruonye

Institute of Urban Innovation, Yokohama National University, 79-5 Tokiwadai Hodogaya-Ku, Yokohama, Japan

A R T I C L E I N F O

Article history :

Received : 8 December 2021

Revised : 18 December 2022

Accepted : 6 March 2023

Keywords:

Durability of concrete

Non-destructive testing

Coefficient of surface water absorption

Coefficient of air permeability

Quality control

A B S T R A C T

Surface Water Absorption Test (SWAT) has long been proposed as a non-destructive testing device for evaluation and grading of the quality of the cover concrete and standardization of SWAT is still in process. In this study, the acceptability and validity of a new water sorptivity index of the SWAT method - the coefficient of surface water absorption (CSWA), are appraised by a correlative assessment between CSWA and the coefficient of air permeability (kT values) measured by the Torrent's double chamber air permeability device. The tests were conducted on fourteen different kinds of concrete at different ages, produced with three different cement types, four water-to-binder ratios, and four curing conditions. The results revealed a good correlation between CSWA and kT for both the specimens with uniform moisture content and the ones with varying degrees of moisture gradients. The findings validate the CSWA as an effective quality control index during design as well as a durability quantifier for evaluating the water absorption resistance of in-situ concrete structures.

1 Introduction

Most of the damage to reinforced concrete structures is due to a lack of durability rather than a lack of strength. The cover concrete that protects the embedded steel material must be dense and sufficiently thick to limit mass transport of deleterious substances for a concrete structure to be durable [1, 2]. In most situations, the quality and thickness of the cover concrete determine the service life of the structure. For instance, scaling deterioration in a frost-damaged environment starts from the surface of the concrete, so the surface layer concrete must also have sufficient scaling resistance. Because the quality of the cover concrete is impacted not only by the mix composition but also by the concreting works (such as placement, compaction, curing, etc.), it is more practical to test the obtained characteristics on the structure rather than individual cast specimens. This has given rise to the increasing need to evaluate the quality of cover concrete of newly completed and existing

Corresponding author. Tel.: +81-8034156734.
E-mail address: uwazuruonye-nnodim-fy@outlook.com

e-ISSN: 2170-127X,

RESEARCH REVIEW of Sciences and Technologies

structures by non-destructive testing. The quality of the cover concrete can be evaluated based on many properties such as water permeability, air permeability and electrical resistivity [3, 4], etc. Since the deterioration of concrete structures is mostly related to the penetration of water from the surface, studies on evaluating the quality of concrete based on the water penetration resistance have been a primary focus [1-3, 5-12].

Water penetration is largely influenced by the action of capillary pores relating to pore diameters, pore continuity/connectivity, tortuosity, and pore saturation degree. Furthermore, surface tension and viscosity, which are influenced by factors like temperature, contribute a great deal to water penetration [13-15]. For a better understanding of how mass transportation and the relating permeability parameters affect the service life of concrete, many investigations have been conducted [16-19]. The relationship among the permeation rate of water into concrete, mix design, curing and degree of drying was investigated and a simple equation to evaluate the water absorption in concrete was proposed [20]. Sakai et al concluded that 'as long as the amount of aggregate and mineral admixture are common, the sorptivity of concrete can be evaluated with the water-to-binder content, curing and the degree of drying' [20]. Zhang et al. showed from an NMR and MIP results that the porosity of concrete increases with water-binder content [21]. Except for basalt fibre, the inclusion of admixtures can effectively decrease the porosity of concrete [21]. Cement type, curing condition and age have also been found to be significant determinants of chloride-ion penetration, porosity and permeability of the interface transition zone in both mortar and concrete [22-25].

Evaluating the resistance to mass transfer of cover concrete has been performed using many nondestructive testing methods [26-30]. The air permeability method by Torrent [26] is one of the most popular, widely accepted testing methods and already established in the Swiss specification for evaluating the resistance to mass transfer of the cover concrete [1, 31]. Many researchers have reported good correlations between the air permeability coefficient *kT* and several concrete durability parameters, such as the threshold radius from the MIP test [32, 33], and quality variation due to segregation of concrete [34]. Moreover, air permeability has proven to be effective in detecting the carbonation rate of concrete as well as the effects of concrete composition on permeability [4, 35].

The main objective of this paper is to appraise the acceptability of the SWAT method by evaluating the correlation between the newly introduced SWAT index – coefficient of surface water absorption (*CSWA*) and the Torrent's air permeability coefficient (*kT*) based on concrete specimens with variable compositions and properties such as cement types, curing conditions, water-to-binder ratios, moisture conditions, ages at measurement, etc. The second objective of this paper includes evaluating the relationship between *CSWA* and the previous/conventional SWAT indices such as the cumulative water absorption and the rate of water absorption.

2 Evaluation of concrete quality by Surface Water Absorption Test (SWAT)

SWAT (Appendix A1) is a non-destructive and short-term (10 minutes) water absorption measurement device that evaluates the quality of the cover concrete under natural dominant water suction [36, 37]. SWAT was developed by Hosoda and Hayashi [36, 37]. The time for injecting water into the water absorption cup is 10 seconds and the conventional grading index is termed surface water absorption rate (*p*) in $ml/m^2/s$. Surface water absorption rate (*p*) derived its course from the proposition by Levitt [38] on the theoretical derivation for initial surface water absorption (ISA) based on the Poiseuille law that obtains the Poiseuille flow in micropore. The surface water absorption rate at 10 minutes (600 seconds) – p_{600}, is given by at^{-n}, where a is the water absorption rate at 1 second, *t* is time in seconds and n is the reduction factor of the water absorption rate.

Investigations have revealed that the SWAT method is effective in detecting the influence of curing conditions, cement type, water-to-cement ratio, carbonation of concrete, and the effects of microcracks in covercrete quality [5, 36, 37, 39-42]. *CSWA* has a strong positive correlation with the destructive JSCE standard water sorptivity test results [43]. The approach to *CSWA* ($ml/m^2/s^{1/2}$) is the same with sorptivity which is determined from the gradient of the straight line obtained by plotting the cumulative water absorption per unit area against the square root of time [41, 43].

2.1 Fundamentals and influential factors of SWAT method

2.1.1 Water contact area

In a water absorption test, it is necessary to consider the effect of the area where water meets the concrete surface. It is known that if the water contact area is extremely small, water absorption will be affected by the presence of coarse aggregate, and the variation in measured results will increase. The diameter of the water absorption cup of the SWAT method is 80 mm (Appendix A1 (b)), and the water contact area is 5024 mm^2. This satisfies the 5000 mm^2 minimum water contact area recommendation in the ISAT method (BS 1881) [44] proposed by Levitt [38].

2.1.2 Water head and air bubbles

Unlike the Initial Surface Absorption Test – ISAT method (BS 1881) [44], the SWAT system does not require a constant water head throughout the testing time. Because of this system, a previous study investigated the effect of the water head on the measured results in the SWAT test method. The initial water heads were set at 100 mm, 200 mm, 300 mm, and 500 mm. The finding (Figure 1) revealed no significant effect of varying the water head levels on the measured results [45]. Nonetheless, air may be entrapped in the process of injecting water into the water absorption cup. If so, the entrapped air could move up to the calibrated cylinder and escape from the top of the cylinder during testing time, causing a drop in the water level. To eliminate the possibility of such an effect, the structure of the water absorption cup is such that does not easily entrap air. Besides, an effective method of injecting water to eliminate entrapping air such as non-rapid water injection should be devised by the investigator.

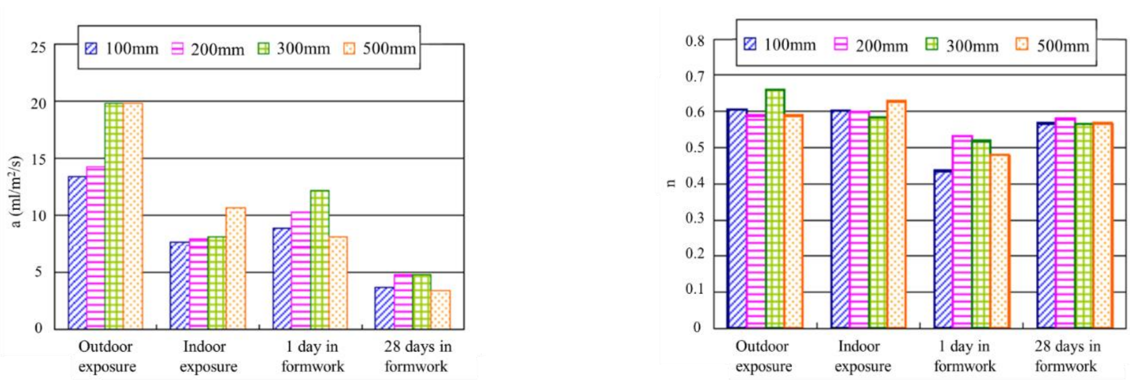

Fig. 1 – Effects of water head on SWAT results. (culled from [45])

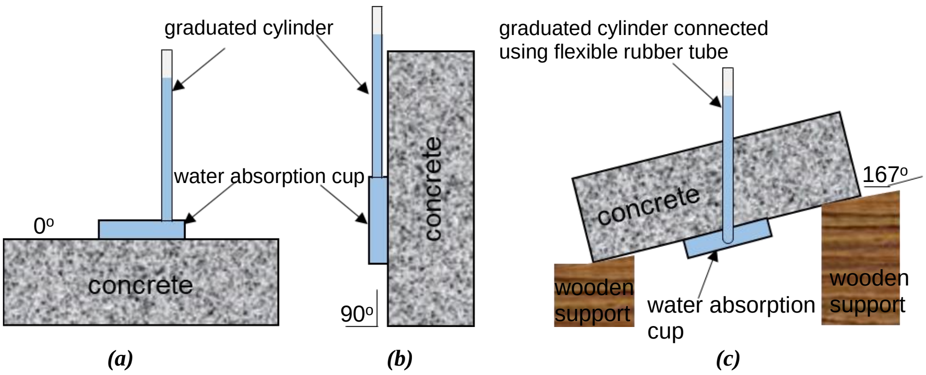

Fig. 2 – Contact angles between water absorption cup and concrete (a) 0 degree (b) 90 degrees (c) 167 degrees

2.1.3 Contact angle of measurement

The effects of three contact angles of measurement (Figure 2) – 0° (top of concrete slab), 90° (vertical face of a concrete wall and 167º (like the shoulder of a tunnel lining) were investigated using ordinary Portland cement concrete – 55% w/c ratio [46]. No effect of these angles on the average amount of absorbed water (ml) and the absorption rate – p_{600} was found (Table 1) and it was concluded that SWAT can be conducted at various angles of the actual concrete structure [46].

Table 1 – Total absorbed water and p_{600} at different angles of measurement (*culled from* [46])

S/n	Contact angle of measurement	Specimen E		Specimen E		Specimen E		Specimen E	
		p_{600} (ml/m^2/s)	Total absorbed water (ml)	p_{600} (ml/m^2/s)	Total absorbed water (ml)	p_{600} (ml/m^2/s)	Total absorbed water (ml)	p_{600} (ml/m^2/s)	Total absorbed water (ml)
1	90º	0.62	2.94	0.54	2.61	0.58	2.86	0.59	2.99
2	90º	0.62	3.01	0.53	2.61	–	–	0.60	2.99
3	0º	0.63	3.06	–	–	–	–	0.63	3.01
4	167º	0.63	3.37	0.62	2.76	0.58	2.81	0.57	2.96

2.1.4 Time-dependent deformation of silicon materials for water tightness and framed vacuum cell

When conducting a non-destructive surface water absorption test, it is necessary to place a sealing material between the water absorption cup and the concrete surface to prevent water leakage. Depending on the method of attaching the water absorption cup and the pressure exerted on the sealing material, continuous deformation during the water absorption test may occur. In such deformation of sealing material, the volume of water inside the absorption cup changes which affects the result of the water absorption test. In the SWAT system, a physical protrusion or stopper is provided in the vacuum cell for installing the frame that holds the water absorption cup on the concrete surface. The frame is fixed by the protrusions meeting the concrete surface to prevent continuous deformation of the sealing material (Figure 3). Also, the type of silicon material is such that does not deform easily and could be readily replaced in any case of deterioration (Figure 3(b)).

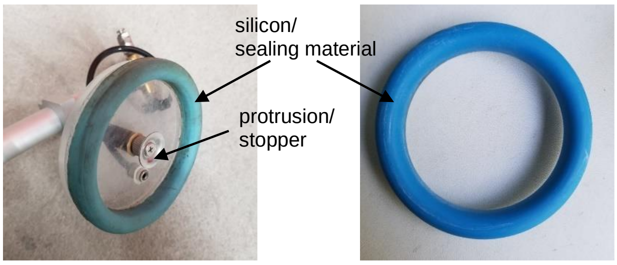

(a) *(b)*

Fig. 3 – Protection system against deformation of sealing material (a) vacuum cell frame, (b) replacement silicone material

2.1.5 Time difference from water injection and the start of measurement

The water absorption rate reaches its maximum immediately after the start of the water absorption test and decreases over time. Since water absorption into concrete starts at the time of contact with concrete before the start of measurement time, changes in the time from the start of water injection to the start of measurement may affect the measurement results. When the total water absorption during the test time or the water absorption rate at a specific time is used as an index, it is necessary to pay attention to this effect. In SWAT, the measurement starting time is 10 seconds after the starting of water injection. Fujiwara et al [45] investigated the effects of changes in time from the start of water injection to the start of measurement on SWAT and confirmed that 10 seconds has no significant effect.

2.1.6 Surface moisture condition

Surface water absorption of in-situ concrete is highly affected by the moisture condition before the measurement due to the existence of moisture gradient and the effects of initial surface moisture contents. Investigations have shown that the effect of moisture content is the greatest challenge and shortcoming for all in-situ cover-concrete measurement devices such as autoclam water/air permeability, double chamber air permeability, electrical resistivity, etc. [3, 47]. SWAT device is not excluded from this challenge as Ngo et al concluded that the effect of moisture content on SWAT is ambiguous [48].

Nonetheless, research advancing the applicability of SWAT by the author [5, 49, 50] have provided in-depth investigations and confirmed the relationship between moisture condition (surface moisture contents and internal moisture gradients) and SWAT results. The reports showed with quantitative values, the region (plateau region) where the degree of saturation of concrete has virtually no effect on the measured results of SWAT (shown in Figure 4). With a multi-scale thermo-hygro dynamic numerical simulation tool, it was further confirmed that the plateau region is composed of finer non-continuous capillary pores, hence, evaluates the connectivity and continuity of the pore system in concrete [5]. The plateau region was propounded as the initial surface moisture contents for effective evaluation of water resistance properties of concrete when using SWAT [5, 49, 50]. This has been successfully applied by other researchers in evaluating the quality of concrete and quantitative grading of in-situ concrete structures [51, 52].

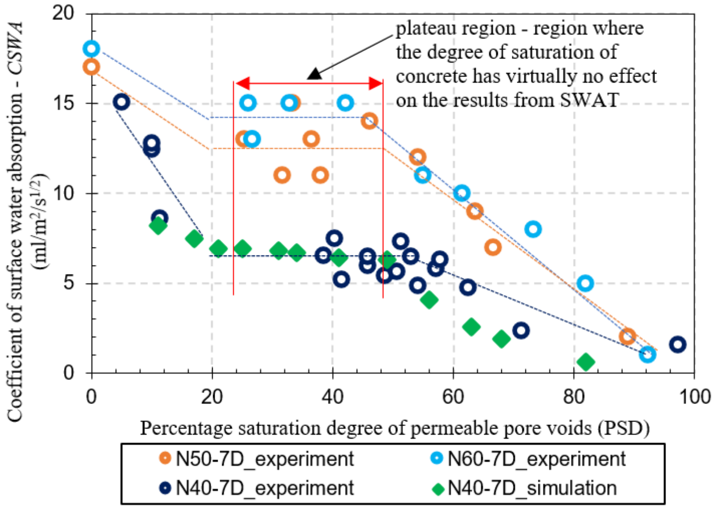

Fig. 4 – Effects of surface moisture content on SWAT results (culled from [46])

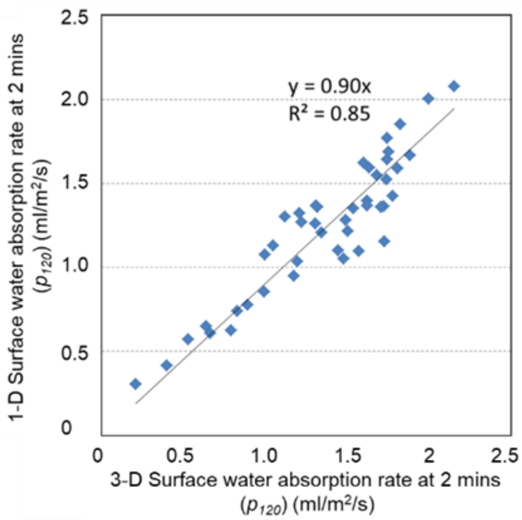

Fig. 5 – 3-D versus 1-D surface water absorption rate (culled from [2])

2.1.7 Three-dimensional and one-dimensional water ingress

When a water absorption test is performed on the surface of a concrete structure, the water absorption phenomenon is always in 3-dimensions. There is concern about the difference from the situation where water absorption is dominant in one dimension. For this reason, surface water absorption tests were performed at various locations on the surface of a full-scale column test structure and concrete cores sampled from the test structure with adequate consideration of the moisture condition to investigate the 3-D and 1-D effects [2]. Figure 5 shows the result for water absorption rates at 2 minutes [2]. Compared to the 3-D water absorption rate performed on the surface of the structure, the 1-D absorption rate measured on the collected core is about 0.9 times, which was concluded to be a small difference. The reason why the difference is small is that the water contact area of the SWAT system is large enough [2].

Table 2 – Concrete mix proportion

s/n	Name of specimen	w/c (%)	w/b (%)	s/a (%)	Mix composition (kg/m^3)						Admixture (%)	
					Water	OPC	BB	FA	Fine aggregate	Coarse aggregate	Ad	AE
1	N40-1D	40	–	45.0	160	400	–	–	777	950	1.0	0.1875
2	N40-7D	40	–	45.0	160	400	–	–	777	950	1.0	0.1875
3	N40-7W	40	–	45.0	160	400	–	–	777	950	1.0	0.1875
4	N50-1D	50	–	47.0	160	320	–	–	841	950	1.0	0.1985
5	N50-7D	50	–	47.0	160	320	–	–	841	950	1.0	0.1985
6	N50-7W	50	–	47.0	160	320	–	–	841	950	1.0	0.1985
7	N60-1D	60	–	48.5	160	267	–	–	890	945	1.0	0.3000
8	N60-7D	60	–	48.5	160	267	–	–	890	945	1.0	0.3000
9	N60-7W	60	–	48.5	160	267	–	–	890	945	1.0	0.3000
10	N40-28D	40	–	45.0	160	400	–	–	796	973	1.0	0.0015
11	N50-28D	50	–	47.0	160	320	–	–	865	975	1.0	0.0015
12	N60-38D	60	–	48.5	160	267	–	–	913	970	0.8	0.0015
13	BB50-28D	50	–	46.7	160	–	320	–	854	975	0.8	0.0015
14	FA41-28D	50	41.6	47.7	154	308	–	62	827	975	1.0	0.0045

N: ordinary Portland cement, BB: ground granulated blast furnace slag cement (JIS type B slag cement), FA: fly ash (JIS type II)
Admixture types, Ad: water-reducing admixture, AE: Air entraining agent
Admixture dosage: percentage of admixtures to the binder, weight-to-weight ratio

3 Experimental programme

3.1 Materials

Concrete specimens were prepared using ordinary Portland cement (OPC) (as per JIS R 5210 [53]), blast furnace slag type B cement (BB) (as per JIS R 5211 [54]) and type II fly ash (as per JIS A 6201 [55]). The fine aggregate used was natural silica pit sand and aggregate was crushed gravel of a 20 mm maximum size. An air-entraining agent (AE) and water-reducing admixtures (Ad) were used for all the concrete. Tap water was used for the mixing.

3.2 Specimen specifications and pre-test conditioning

For this study, two different sizes of concrete specimens were cast following fourteen mixtures given in Table 2. The concrete prisms were cured in several conditions to obtain variations in quality that will cover both poor and good quality. The age of concrete at measurement was varied to obtain both young and matured concrete. Two experimental series, I and II were systematically conducted to include the effects of several moisture conditions. The concrete materials, size, mixtures, and pre-test conditions/preparations for the experimental series I and II are discussed in 3.2.1 and 3.2.2 respectively.

3.2.1 Specimens with internal moisture gradient (series I)

A set of concrete specimens measuring 300 mm x 150 mm thickness x 300 mm height (Figure 6) was prepared to investigate *CSWA* and *kT* on specimens with several kinds of internal moisture gradients and varying surface moisture contents. In the set, 9 concrete mix designs of ordinary Portland cement (OPC) were prepared with the mixture proportions ~ serial number (s/n) 1 – 9 in Table 2. The water-to-cement contents were 40%, 50%, and 60%. Three curing conditions were adopted. The curing conditions applied were 1D: 1 day in mould, 7D: 7 days in mould, and 7W: 1 day in mould + 6 days in water. The specimens were named N40-1D (OPC + 40% w/c + 1D), N50-1D (OPC + 50% w/c + 1D), N60-1D (OPC + 60% w/c + 1D), N40-7D (OPC + 40% w/c + 7D), N50-7D (OPC + 50% w/c + 7D), N60-7D (OPC + 60% w/c + 7D), N40-7W (OPC + 40% w/c + 7W), N50-7W (OPC + 50% w/c + 7W), and N60-7W (OPC + 60% w/c + 7W). Six specimens were prepared for each mix design with M4 threaded electrode moisture sensors embedded (in pairs) in 3 specimens at different locations from the surface. The M4 threaded electrode moisture sensors were embedded at 5 mm, 10 mm, 20 mm, 30 mm, and 50 mm from the surface of the concrete to confirm the existence of internal moisture gradients prior to tests. The specimens were kept in a controlled room ~ 20ºC and 60% relative humidity until 60 days after the placing of the concrete.

Figure 7 details the experimental procedure for specimens in series I. At 60 days after placement, the prismatic specimens were moved to 3 different relative humidity (RH) conditions (60%, 80% and 99.9%) for 1 or 2 days before starting measurements. One specimen without an M4 sensor and one specimen with embedded M4 sensors from each mix design were moved to each of the RH conditions. Test measurements were conducted every 2 days.

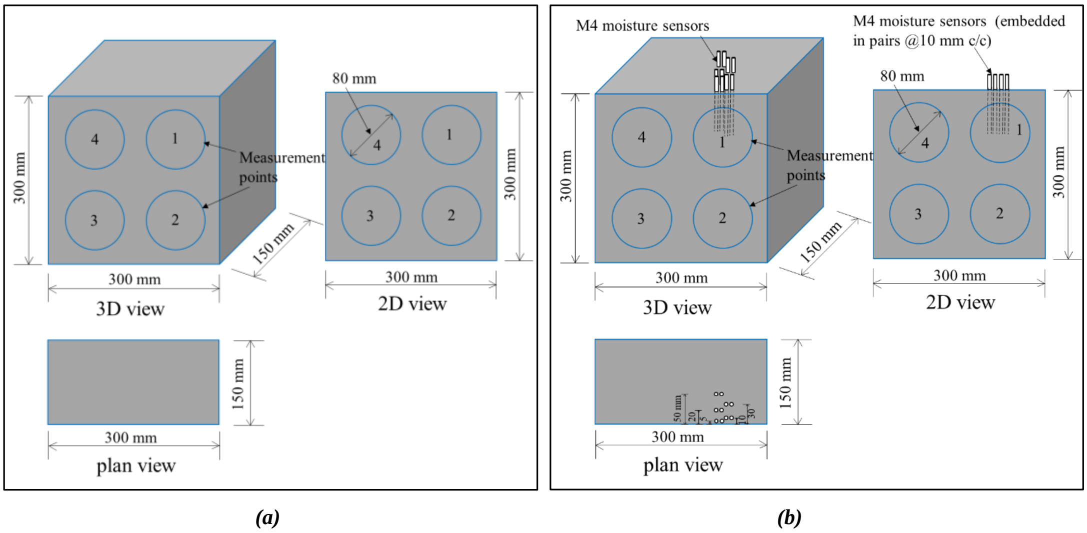

Fig. 6 – Prismatic concrete specimens with internal moisture gradient (a) without M4 moisture sensor, (b) with M4 moisture sensors

3.2.2 Specimens preconditioned to uniform moisture contents (series II)

A set of concrete prisms measuring 100 mm x 75 mm thickness x 100 mm height (Figure 8) was prepared to investigate *CSWA* and *kT* on specimens with different degrees of uniform internal moisture and surface moisture contents. This specimen size was selected to achieve equilibrium moisture conditions during preconditioning based on previous reports and works on literature [50, 56]. Two cement types were used: ordinary Portland cement (OPC) and ground granulated blast furnace slag cement (JIS type B slag cement). Also, JIS type II fly ash (FA) was used as supplementary cementitious material (SCM) replacing fine aggregate at 20% by volume of OPC. Five types of concrete were prepared with the mixture proportions ~ serial number (s/n) 10 – 14 in Table 2. The water-to-binder contents were 40%, 41.6%, 50%, and 60%. The curing applied was 28 days in mould/sealed condition and the specimens were named: N40-28D (OPC + 40% w/c), N50-28D (OPC + 50% w/c), N60-28D (OPC + 60% w/c), BB50-28D (BB + 50% w/c) and FA41-28D (OPC + FA + 41.6% w/b). Twelve concrete prisms were prepared for each mix design and were preconditioned to equilibrium moisture contents at several degrees. Six prisms were prepared without M4 sensors for air permeability test while M4 threaded electrode moisture sensors were embedded in 6 prisms for surface water absorption tests. The M4 threaded electrode moisture sensors were embedded (in pairs) at different locations from the surface (5 mm, 25 mm, 37 mm, and 45 mm) to monitor the moisture profile during preconditioning (Figure 8(b)). To ensure sufficient hydration and avoid change in the microstructure due to preconditioning, the specimens were kept in a controlled room (20ºC and 60% RH) until 152 days before starting preconditioning and testing, which lasted until 540 days from the time of placement.

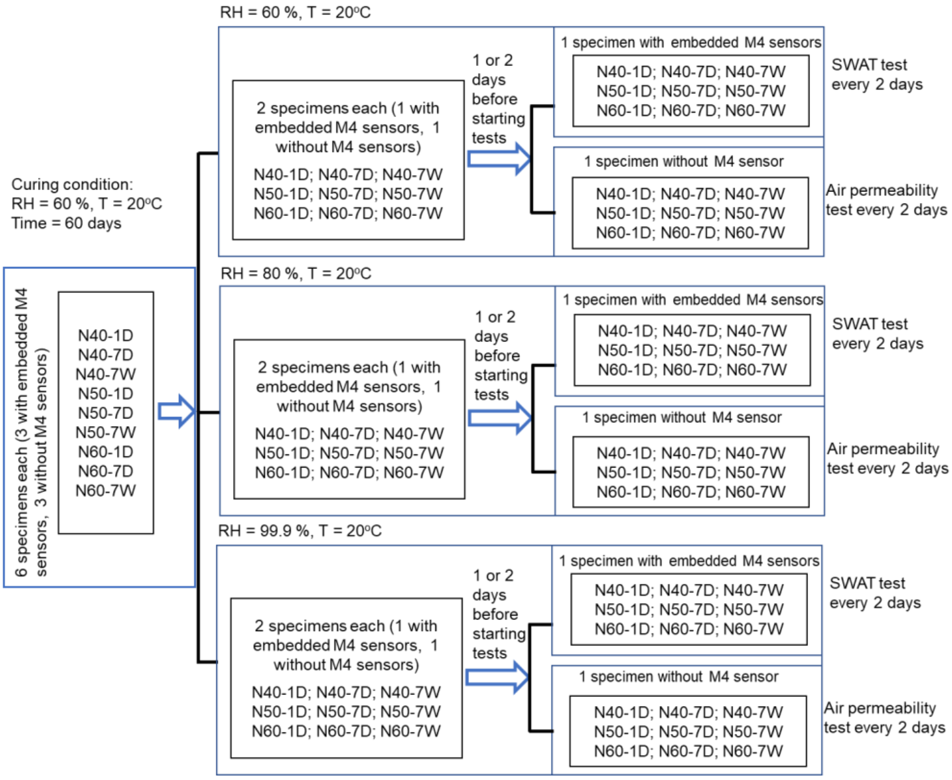

Fig. 7 – Experimental steps for series I specimens

To reduce preconditioning time while covering several degrees of equilibrium moisture condition and surface moisture contents, the preconditioning of the specimens was done in two ways – desorption (wet-to-dry) and absorption (dry-to-wet) processes. Besides the steps also appraised the effects of hysteresis on the test results, which, however, is not within the scope of this paper.

(a) Preconditioning to moisture equilibrium at different moisture contents through a desorption process

For wet-to-dry preconditioning (desorption process), 3 specimens with sensors and 3 without sensors were saturated by total immersion into water after which stepwise drying and moisture re-distribution was carried out. The steps for preconditioning the specimens, which has been previously established by the author [50], is summarised below:

- Saturating specimen by total immersion into water.
- Sealing four sides with vinyl electric insulation tape to eliminate multi-lateral moisture transfer during conditioning [57]. This enables unilateral and easy moisture redistribution to obtain uniform moisture content in the concrete.
- Drying the specimen for 6 hours in a controlled chamber (40°C, 50% RH).
- Sealing the two faces of the specimens with a layer of polythene sheet.
- Returning the specimen to the controlled chamber (40°C, 50% RH) to allow for moisture redistribution and attainment of uniform moisture.
- Storing the specimen in a different enclosed chamber to allow for natural heat loss until a temperature between 20 - 25oC is reached.

(b) Preconditioning to moisture equilibrium at different moisture contents through an absorption process

To precondition the specimens and obtain equilibrium moisture at different moisture contents using an absorption process (dry-to-wet), the pore void was emptied to the lowest possible degree by drying at a temperature of 40°C. This temperature was selected to ensure that only the pore water was removed and to avoid generating microcracks. Three specimens with embedded sensors and 3 specimens without sensors were used from each mix design. The steps for dry-to-wet preconditioning are:

- Drying the specimen to a steady weight in a chamber at a temperature of 40°C
- Sealing four sides with vinyl electric insulation tape to eliminate multi-lateral moisture transfer. This enables unilateral and easy moisture redistribution to obtain uniform moisture content in the concrete.
- Immersing specimen into water for 15 minutes.
- Drying faces with a towel.
- Sealing the two faces of the specimens with a layer of polythene sheet.
- Putting the specimen into a controlled chamber (40°C, 50% RH) to allow for moisture redistribution and attainment of uniform moisture.
- Storing the specimen in a different enclosed chamber to allow for natural heat loss until a temperature between 20 - 25°C is reached.

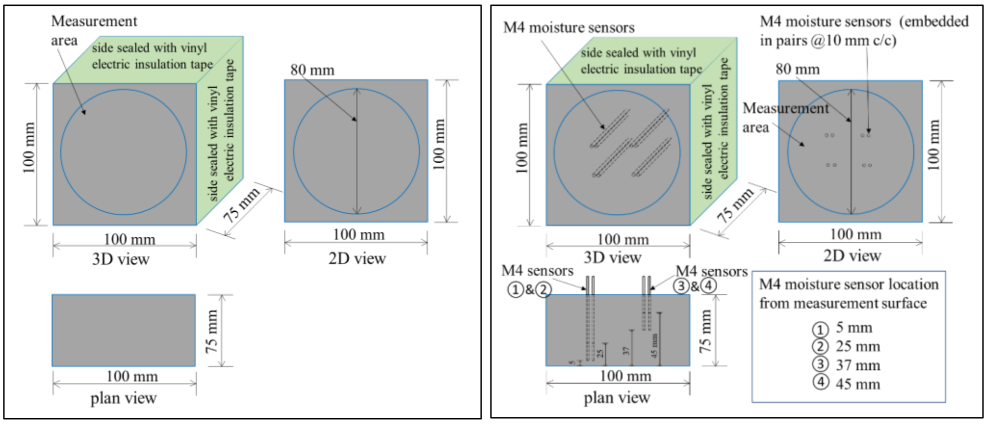

(a) *(b)*

Fig. 8 – Prismatic concrete specimens preconditioned to uniform moisture contents: (a) without M4 moisture sensor (b) with M4 moisture sensors

3.3 Test methods and measurements

Surface moisture contents for both series of concrete specimens were measured with the electrical impedance moisture meter – CMEX II, Tramex Ltd, Ireland. The moisture meter was selected because the relationship with Torrent's air permeability is well known. Also, the threshold for effective air permeability evaluation has already been established [31]. The internal moisture of the concrete specimens was measured by attaching the electrical resistivity moisture meter – HI-800, Kett Electric Laboratory, Japan to the embedded M4 moisture sensors.

Air permeability test was conducted utilizing the commercial Torrent method (PermeaTORR AC model). The air permeability method by Torrent has long been established as a Swiss standard- Swiss Standard SIA 262, "Concrete Structures" [34]. The device automatically calculates the air permeability coefficient - kT (in 10^{-16}m2) employing an inbuilt model [26, 35] which is computed by the following numerical formula – Eq. 1, and the maximum penetration depth L of the Pa front is calculated by Eq. (2).

$$kT = \left(\frac{V_c}{A_{in}}\right)^2 * \frac{\mu}{2\varepsilon P_a}\left[\frac{\ln\left(\frac{P_a + \triangle P_i}{P_a - \triangle P_i}\right)}{\sqrt{t_f} - \sqrt{t_0}}\right]^2 (m^2) \quad (1)$$

$$L = \left(\frac{2kTP_a t_f}{\varepsilon\mu}\right)^{\frac{1}{2}} \quad (2)$$

where V_c: volume of the inner cell system (m^3), A_{in}: cross-sectional area of the inner cell (m^2), μ: viscosity of air (=2.0 *10^{-5} N.s/m^2), $\mathcal{E}$: estimated porosity of covercrete (=0.15), P_a: atmospheric pressure (Pa = N/m2), $\triangle P_i$: pressure rise in the inner cell at time t_f (Pa = N/m^2), t_f: time (s) at the end of the test (=360 s), t_0: time (s) at the beginning of the test (=60 s)

To ensure airtightness during measurements a clear perforated acrylic plate with a rubber seal (Figure 9) was used. For series I, air permeability was conducted with moisture measurements on specimens without embedded M4 moisture sensors and average results of four measurement points (shown in figure 6(a)) were used for the analysis. Also, air permeability was conducted with moisture measurements on three replicate concrete prisms without embedded M4 moisture sensors for the series II specimens (Figure 8(a)) and the average results were used.

Surface water absorption was conducted with moisture measurements on four measurement points (Figure 6(b)) of the series I specimens with embedded M4 moisture sensors. The average *CSWA* deduced from the measurements was used for the analysis. For series II, the average *CSWA* obtained from three measurements on replicate prisms was used.

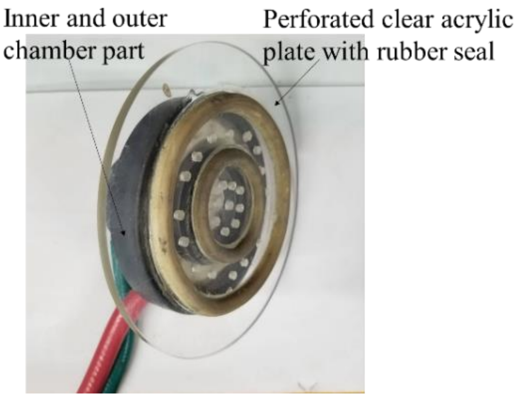

Fig. 9 – Clear and perforated acrylic plate with rubber seal

4 Results and discussions

4.1 Moisture conditions before tests

The surface moisture contents of the specimens cover both wet and dry concretes as shown in Figure 10. Surface moisture contents for series I specimens (Figure 10(a)) range from 4.5% to 6.8% while that of series II (Figure 10(b)) ranges from 0% to 6.9%. Just as expected, specimens exposed to 99.9% RH exhibited higher surface moisture contents (above 5.5% and increase up to 6.9% with the passage of days) as the samples preconditioned through the desorption process (wet-to-dry path) at the beginning and decrease down to 4.4% with the stepwise desorption preconditioning. The series I specimens exposed to 60% and 80% RH showed surface moistures between 4.5% to 5.8% while the series II specimens preconditioned by the absorption process (dry-to-wet path) showed surface moistures between 0% to 3.8%. Although the initial surface moisture contents for some specimens were above the upper thresholds for both Torrent's permeability test [31] and SWAT [50], the obtained *kT* and *CSWA* values were not excluded from the correlative analysis since Torrent's test and SWAT have different upper threshold values. This is also to provide an inclusive correlative evaluation that will accommodate the complex effects of initial surface moisture contents and internal moisture gradients like structures in outdoor exposure.

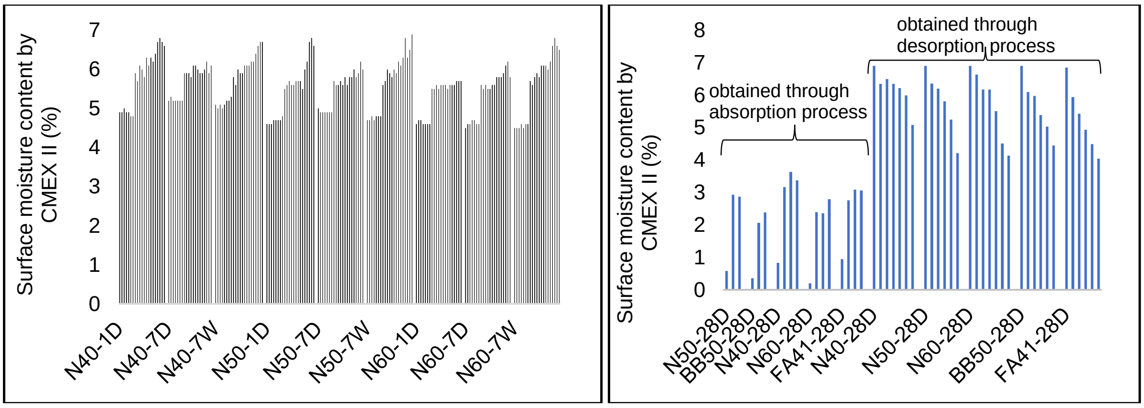

(a) *(b)*

Fig. 10 – Variations in surface moisture content of concrete before tests by CMEX II moisture meter, (a) specimens with internal moisture gradients (b) specimens preconditioned to uniform moisture content

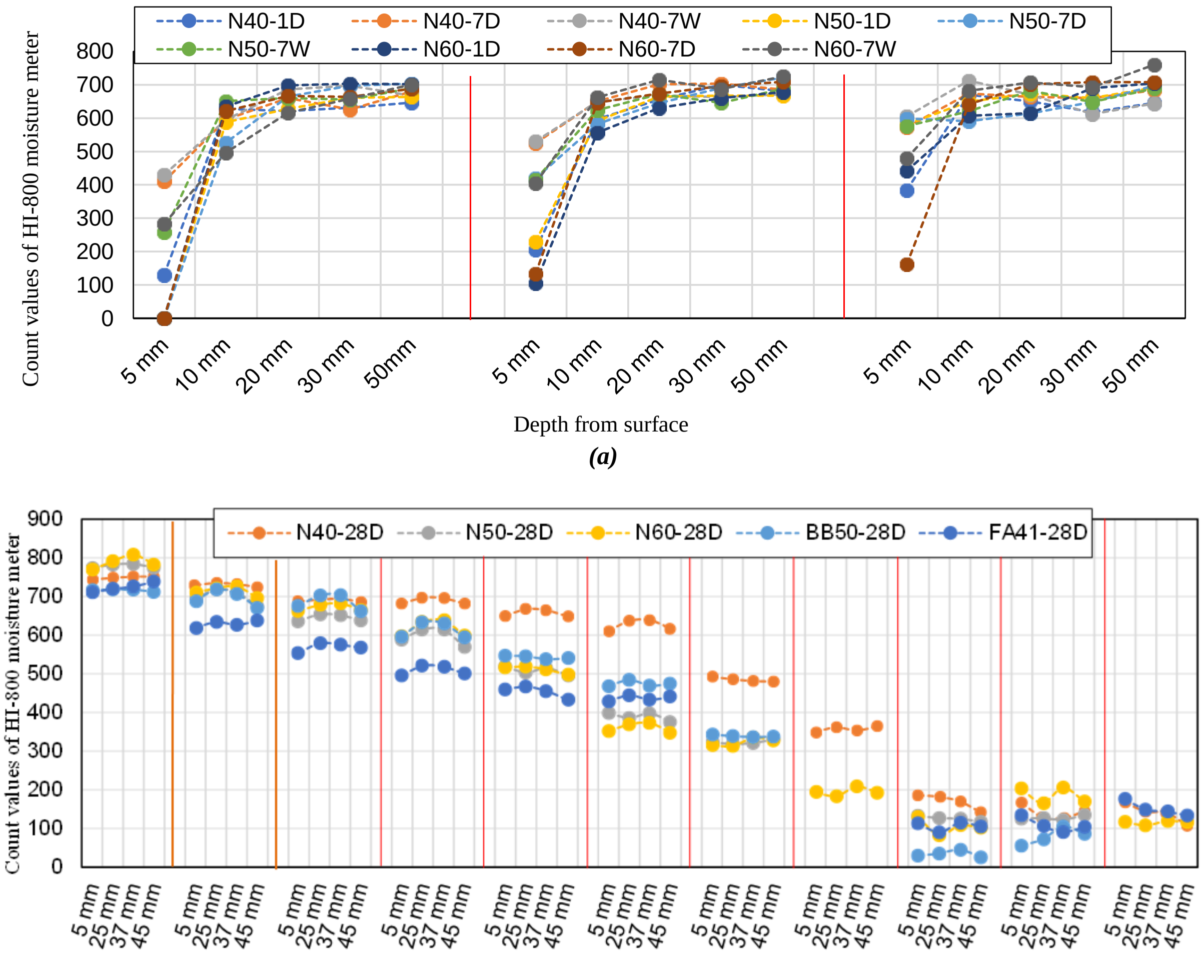

(a)

(b)

Fig. 11 – Typical moisture distribution across the depth of concrete before tests by Kett HI-800: (a) specimens with internal moisture gradients (b) specimens preconditioned to uniform moisture content

Figure 11(a) shows typical internal gradients of the series I specimens while Figure 11(b) shows the internal moisture distributions of the series II specimens. It can be seen from Figure 11(a) that exposing the concrete prisms to 60%, 80% and 99.9% RH conditions generated several kinds and degrees of internal moisture gradients, which were measured at 5 mm, 10 mm, 20 mm, 30 mm, and 50 mm across the 150 mm thickness. Just as expected, moisture content increases with an increase in the depth from the surface. The highest slope is between 5 mm and 10 mm depths and almost the same degree of moisture at 30 mm and 50 mm depths for all the concrete types. Furthermore, the moisture contents from the cover zone to 10 mm depth, which could be explained as the most influential depth on the test measurements, cover both wet and dry conditions. Figure 11(b) is the confirmation of uniform moisture contents that were measured at 5 mm, 25 mm, 37 mm, and 45 mm from the surface of the preconditioned concrete specimens (at different times and for many degrees of saturation) across the 75 mm thickness.

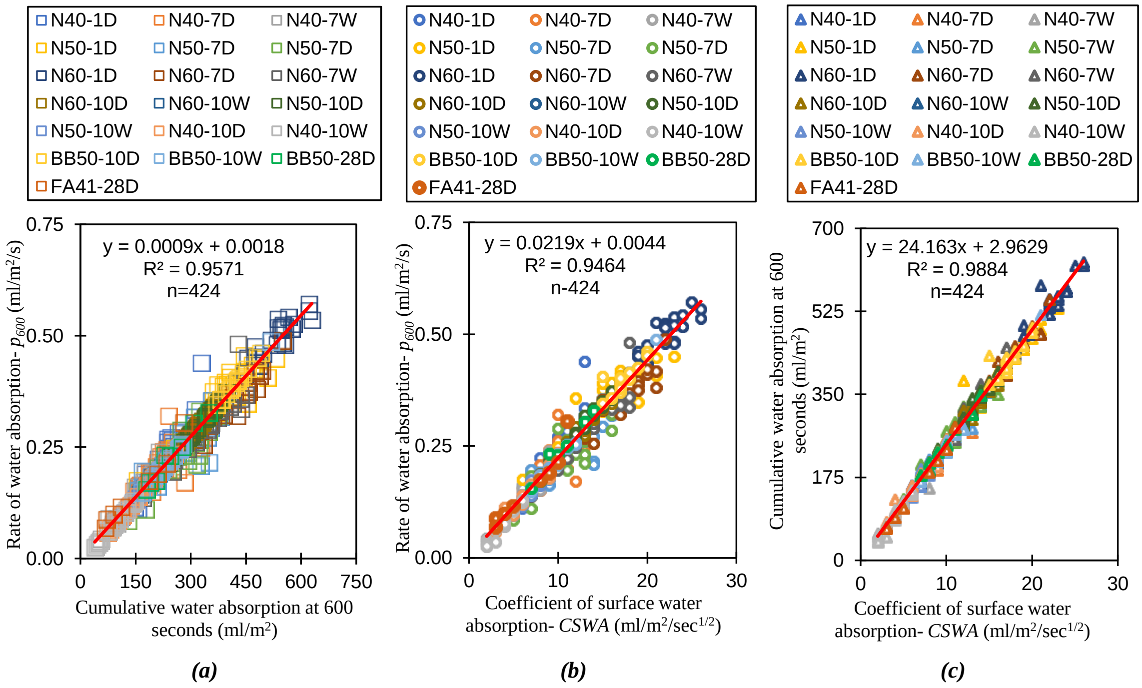

Fig. 12 – Relationship between SWAT indices (a) p_{600} versus cumulative water absorption at 600 seconds, (b) p_{600} versus CSWA (c) cumulative water absorption at 600 seconds versus CSWA

4.2 Relationships between SWAT evaluation indices

The relationships between different SWAT indices (the rate of water absorption versus cumulative water absorption, rate of water absorption versus coefficient of surface water absorption, cumulative water absorption versus coefficient of surface water absorption) are shown in Figure 12. For a more comprehensive evaluation, additional SWAT data from previous investigations (for concrete samples with internal moisture gradients, composed of variable curing conditions, cement types, specimen sizes, and ages at measurement) were added to the measurement results of the series I specimens of this study and utilized for the analysis.

For a good system of quality evaluation of concrete, it is known that the use of the cumulative absorbed water during the test, which is the most easily obtained index even by short-time measurement, is paramount. Nonetheless, care must be taken as this index may easily be affected by the difference between the water injection time and the start of measurement time. It could be inferred in Figure 12(a) that p_{600} has a positive and high correlation with cumulative water absorption like for figures 12(b) and 12(c) which revealed positive and strong coefficients of determination for the relationships between p_{600} and *CSWA*, and cumulative water absorption and *CSWA* respectively.

4.3 Variation in test measurement time

As earlier mentioned, it is also necessary to consider the test measurement time for appropriately evaluating the water absorption resistance of concrete. It was reported that in a relatively short water absorption test of about 10 minutes, there is a correlation between the indices showing water absorption resistance obtained at different measurement times. For this reason, the collection of the measurement results explained in section 4.2 above were applied to evaluate the influence of test measurement time. Figure 13 shows the plot of water absorption rate at 10 minutes (p_{600}) versus water absorption rate at 2 minutes (p_{120}). As seen in the figure, a high correlation between p_{600} *and* p_{120} is confirmed. It validates that in the surface water absorption test of 10 minutes, the measurement time can be shortened without affecting the judgement of the measured water resistance properties.

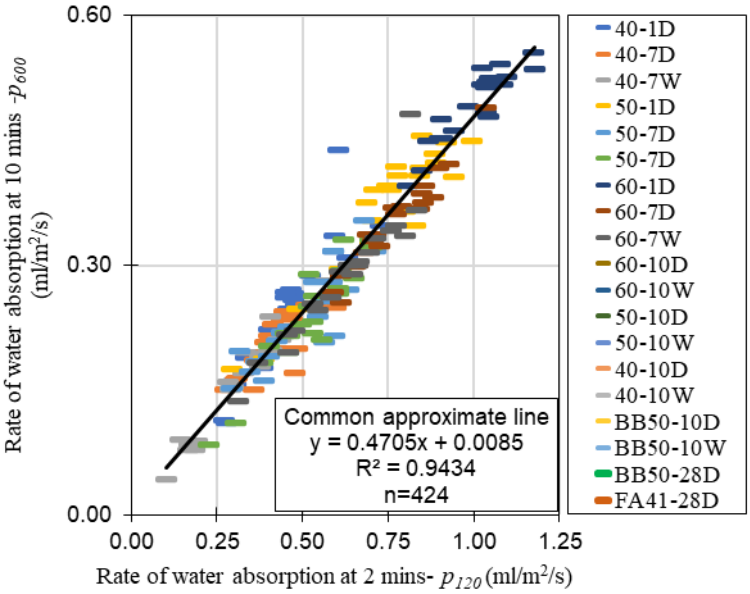

Fig. 13 – Relationship between rate of water absorption at 10 mins (p_{600}) and rate of water absorption at 2 mins (p_{120})

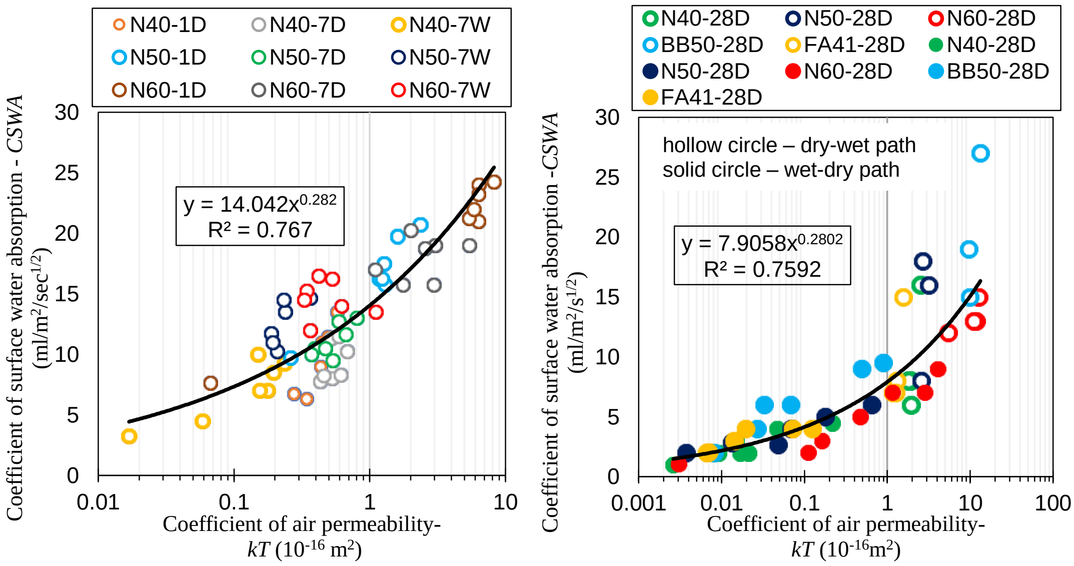

(a) *(b)*

Fig. 14 – Relationship between kT and CSWA values (a) concrete specimens with internal moisture gradients, (b) concrete specimens preconditioned to uniform moisture content

4.4 Relationship between kT and CSWA

The average values of *kT* and *CSWA* obtained from concrete specimens with both internal moisture gradients and uniform moisture distributions are shown in Figure 14. Figure 14(a) shows the results for specimens with internal moisture gradients while Figure 14(b) is for the specimens preconditioned to uniform moisture content. The results revealed a strong positive relationship between *kT* and *CSWA*. For specimens with internal moisture gradients, a high coefficient of determination - R^2 = 0.767, was obtained for the approximation of the relationship by a power equation like for the specimens preconditioned to uniform moisture distribution which revealed a coefficient of determination - R^2 = 0.7592. This high correlation validates the acceptability of the SWAT for evaluating the transport properties of cover concrete.

5 Conclusions

This study investigated the coefficient of surface water absorption (*CSWA*) measured by the Surface Water Absorption Test (SWAT) and air permeability coefficient (*kT*) measured by the Torrent's double chamber air permeability test of concrete specimens at ages between 60 days to 540 days, produced with different cement types, water-to-binder ratios, curing types/periods, and conditioned to many kinds of complicated moisture conditions exhibiting both internal moisture gradient and equilibrium moisture contents. The results were analysed to validate *CSWA* as a quality grading parameter for non-destructive testing of cover concrete. The summary of the findings and the conclusions obtained from the study revealed a strong positive correlation between *kT* and *CSWA*. High coefficients of determination were obtained by approximate power functions of the relationships for concrete specimens with internal moisture gradients and the ones preconditioned to uniform moisture contents. The strong positive correlation validates the usability and acceptability of the *CSWA* SWAT index in evaluating the resistance to mass transport properties of concrete at the cover zone. Furthermore, there are strong positive correlations between SWAT evaluation indices. High coefficients of determination were obtained by approximate linear functions of the relationships between cumulative water absorption (ml/m^2) and rate of water absorption at 10 minutes (p_{600}), cumulative water absorption (ml/m^2), and coefficient of surface water absorption-*CSWA* (ml/m^2/s$^{1/2}$), as well as the rate of water absorption at 10 minutes (p_{600}) and coefficient of surface water absorption-*CSWA* (ml/m^2/s$^{1/2}$). This validates that any of the three indices could be effectively applied to evaluate the water-resistance properties of concrete. Also, a strong positive correlation between the rate of water absorption at 10 minutes (p_{600}) and the rate of water absorption at 2 minutes (p_{120}). It validates that in the surface water absorption test of 10 minutes, the measurement time can be shortened without affecting the judgement of the measured water resistance properties.

REFERENCES

[1]- R. Torrent, E. Denarié, F. Jacobs, A. Leemann, T. Teruzzi, Specification and site control of the permeability of the cover concrete: The Swiss approach. Materials and Corrosion, 63(12) (2012) 1127-1133. doi:10.1002/maco.201206710.

[2]- A. Hosoda, Quality evaluation method for concrete structures utilizing non-destructive absorption test. Non-destructive Inspection, 70 (3) (2021).

[3]- A.E. Long, G.D. Henderson, F.R. Montgomery, Why assess the properties of near-surface concrete? Construction and Building Materials, 15(2) (2001) 65-79. doi:10.1016/S0950-0618(00)00056-8.

[4]- K. Nakarai, K. Shitama, S. Nishio, Y. Sakai, H. Ueda, T. Kishi, Long-term permeability measurements on site-cast concrete box culverts. Construction and Building Materials, 198 (2019) 777-785. doi:10.1016/j.conbuildmat.2018.11.263.

[5]- R.N. Uwazuruonye, A. Hosoda, Numerical simulation of water sorptivity of concrete measured by Surface Water Absorption Test. Evaluation, 2 (2021) 1295-1300.

[6]- X. Pan, Z. Shi, C. Shi, T.-C. Ling, N. Li, A review on concrete surface treatment Part I: Types and mechanisms. Construction and Building Materials, 132 (2017) 578-590. doi:10.1016/j.conbuildmat.2016.12.025.

[7]- S. Bouharoun, Characterization of the interface between fresh concrete and formwork. Journal of Civil Engineering and Management, 22(1) (2016) 26-37. doi:10.3846/13923730.2014.893912.

[8]- A. Amriou, M. Bencheikh, New experimental method for evaluating the water permeability of concrete by a lateral flow procedure on a hollow cylindrical test piece. Construction and Building Materials, 151 (2017) 642-649. doi:10.1016/j.conbuildmat.2017.06.126.

[9]- Ł. Sadowski, T.G. Mathia, Multi-scale metrology of concrete surface morphology: Fundamentals and specificity. Construction and Building Materials, 113 (2016) 613-621. doi:10.1016/j.conbuildmat.2016.03.099.

[10]- Z. Cui, A. Alipour, Concrete cover cracking and service life prediction of reinforced concrete structures in corrosive environments. Construction and Building Materials, 159 (2018) 652-671. doi:10.1016/j.conbuildmat.2017.03.224.

[11]- M.H.F. Medeiros, P. Helene, Surface treatment of reinforced concrete in marine environment: Influence on chloride diffusion coefficient and capillary water absorption. Construction and Building Materials, 23(3) (2009) 1476-1484. doi:10.1016/j.conbuildmat.2008.06.013.

[12]- A.M. Neville, Properties of concrete. Vol. 4. Longman London, 2004.

[13]- C. Hall, Water sorptivity of mortars and concretes: a review. Magazine of Concrete Research, 41(147) (1989) 51-61. doi:10.1680/macr.1989.41.147.51.

[14]- R.J. Gummerson, C. Hall, W.D. Hoff, Water movement in porous building materials—II. Hydraulic suction and sorptivity of brick and other masonry materials. Building and Environment, 15(2) (1980) 101-108. doi:10.1016/0360-1323(80)90015-3.

[15]- A.F. Castro, M. Valcuende, B. Vidal, Using microwave near-field reflection measurements as a non-destructive test to determine water penetration depth of concrete. NDT & E International, 75 (2015) 26-32. doi:10.1016/j.ndteint.2015.06.003.

[16]- A.P.B. Capraro, M.A. Cheremeta, M.P.G. Gonçalves, C. Cremonez, M.H.F. de Medeiros, Influence of the cement type and water/cement ratio in concretes exposed in sewage treatment plants. Construction and Building Materials, 229 (2019) 116842. doi:10.1016/j.conbuildmat.2019.116842.

[17]- L.G. Baquerizo, T. Matschei, K.L. Scrivener, Impact of water activity on the stability of ettringite. Cement and Concrete Research, 79 (2016) 31-44. doi:10.1016/j.cemconres.2015.07.008.

[18]- H. Ueda, Y. Sakai, K. Kinomura, K. Watanabe, T. Ishida, T. Kishi, Durability Design Method Considering Reinforcement Corrosion due to Water Penetration. Journal of Advanced Concrete Technology, 18(1) (2020) 27-38. doi:10.3151/jact.18.27.

[19]- R. He, H. Ma, R.B. Hafiz, C. Fu, X. Jin, J. He, Determining porosity and pore network connectivity of cement-based materials by a modified non-contact electrical resistivity measurement: Experiment and theory. Materials & Design, 156 (2018) 82-92. doi:10.1016/j.matdes.2018.06.045.

[20]- Y. Sakai, Y. Yokoyama, T. Kishi, Relationship Among the Permeation Rate of Water into Concrete, the Mix Design, Curing, and the Degree of Drying. Journal of Advanced Concrete Technology, 15(10) (2017) 595-602. doi:10.3151/jact.15.595.

[21]- J. Zhang, F. Bian, Y. Zhang, Z. Fang, C. Fu, J. Guo, Effect of pore structures on gas permeability and chloride diffusivity of concrete. Construction and Building Materials, 163 (2018) 402-413. doi:10.1016/j.conbuildmat.2017.12.111.

[22]- E. Güneyisi, M. Gesoğlu, T. Özturan, E. Özbay, Estimation of chloride permeability of concretes by empirical modeling: Considering effects of cement type, curing condition and age. Construction and Building Materials, 23(1) (2009) 469-481. doi:10.1016/j.conbuildmat.2007.10.022.

[23]- B. Liu, J. Jiang, S. Shen, F. Zhou, J. Shi, Z. He, Effects of curing methods of concrete after steam curing on mechanical strength and permeability. Construction and Building Materials, 256 (2020) 119441. doi:10.1016/j.conbuildmat.2020.119441.

[24]- A.A. Ramezanianpour, V.M. Malhotra, Effect of curing on the compressive strength, resistance to chloride-ion penetration and porosity of concretes incorporating slag, fly ash or silica fume. Cement and Concrete Composites, 17(2) (1995) 125-133. doi:10.1016/0958-9465(95)00005-W.

[25]- X. Sun, B. Zhang, Q. Dai, X. Yu, Investigation of internal curing effects on microstructure and permeability of interface transition zones in cement mortar with SEM imaging, transport simulation and hydration modeling techniques. Construction and Building Materials, 76 (2015) 366-379. doi:10.1016/j.conbuildmat.2014.12.014.

[26]- R.J. Torrent, A two-chamber vacuum cell for measuring the coefficient of permeability to air of the concrete cover on site. Materials and Structures, 25(6) (1992) 358-365. doi:10.1007/BF02472595.

[27]- P. Basheer. Clam'tests for assessing the durability of concrete. PhD thesis, Dep. of Civil Engineering, The Queens University of Belfast, 1991.

[28]- O. Sengul, Use of electrical resistivity as an indicator for durability. Construction and Building Materials, 73 (2014) 434-441. doi:10.1016/j.conbuildmat.2014.09.077.

[29]- F. Wenner, A method of measuring earth resistivity. US Department of Commerce, Bureau of Standards, 1916.

[30]- A. Hosoda, K. Hayashi. Evaluation of covercrete quality of concrete structures by surface water absorption test. in International Symposium on Concrete Structures for Next Generation – CSN. Japan. (2017), 377-386.

[31]- S.S. Association, Swisscode SIA 262: Concrete structures. , Swiss Society of Engineers and Architects Zurich, Switzerland. (2003).

[32]- Y. Sakai, C. Nakamura, T. Kishi, Correlation between Permeability of Concrete and Threshold Pore Size obtained with Epoxy-Coated Sample. Journal of Advanced Concrete Technology, 11(8) (2013) 189-195. doi:10.3151/jact.11.189.

[33]- Y. Sakai, C. Nakamura, T. Kishi, Evaluation of mass transfer resistance of concrete based on representative pore size of permeation resistance. Construction and Building Materials, 51 (2014) 40-46. doi:10.1016/j.conbuildmat.2013.10.037.

[34]- Y. Kato, Characteristics of the Surface Air Permeability Test and the Evaluation of Quality Variation in Cover Concrete due to Segregation of Concrete. Journal of Advanced Concrete Technology, 11(11) (2013) 322-332. doi:10.3151/jact.11.322.

[35]- M. Romer, Effect of moisture and concrete composition on the torrent permeability measurement. Materials and Structures, 38(5) (2005) 541-547. doi:10.1007/BF02479545.

[36]- K. Hayashi, A. Hosoda, Development of surface water absorption test applicable to actual structures. Proceedings of Japan Concrete Institute, 33(1) (2011) 1769-1774.

[37]- K. Hayashi, A. Hosoda, Fundamental study on evaluation method of covercrete quality of concrete structures by surface water absorption test. Journal of Japan Society of Civil Engineers, Ser. E2 (Materials and Concrete Structures), 69(1) (2013) 82-97. doi:10.2208/jscejmcs.69.82.

[38]- M. Levitt, Non-destructive testing of concrete by the initial surface absorption method, in Non-destructive testing of concrete and timber: London. (1969), 23-26. doi:10.1680/ntocats.44685.0005.

[39]- K. Hayashi, A. Hosoda, U. Akmal, Method for identifying water-cement ratio and curing conditions using surface water absorption test, concrete quality, and durability verification system. Research Subcommittee (335 committee) for the Surface Layer of Structures Book and Symposium Lecture Summary. JSCE Journal, (2012) 651-6565.

[40]- S. Komatsu, R. Tajima, A. Hosoda, Proposal of Quality Evaluation Method for Upper Surface of Concrete Slab with Surface Water Absorption Test. Concrete Research and Technology, 29 (2018) 33-40. doi:10.3151/crt.29.33.

[41]- R.N. Uwazuruonye, A. Hosoda, Investigation on correlation between surface water absorption test and JSCE sorptivity test. Proceedings of Japan Concrete Institute, 42(1) (2020) 1726-1731.

[42]- H.P. Nam, A. Hosoda, Improvement of water and chloride penetration resistance of slag concrete by using high alite cement. Proceedings of the JCI, 37(1) (2015) 661-666.

[43]- M.A. Wilson, M.A. Carter, W.D. Hoff, British standard and RILEM water absorption tests: A critical evaluation. Materials and Structures, 32(8) (1999) 571-578. doi:10.1007/BF02480491.

[44]- B. Standard, BS 1881, Part 207 Testing Concrete. Recommendations for the Assessment of Concrete Strength by Near to surface Tests, London, British Standards Institution London. (1992).

[45]- M. Fujiwara, K. Hayashi, A. Hosoda, U. Akmal, Effect of water head and test start time on surface water absorption test. JSCE Journal, 57 (2011) 113-114. .

[46]- Y. Yokoyama, A. Hosoda, Analysis of Effects of Angle of Measurement on Surface Water Absorption Test. Concrete Research and Technology, 28 (2017) 71-78. doi:10.3151/crt.28.71.

[47]- P.A. Claisse, Transport properties of concrete: Measurements and applications. Woodhead Publishing, Elsevier, 2014.

[48]- V. Ngo, A. Hosoda, S. Komatsu, N. Ikawa, Effect of moisture content on surface water absorption test and air permeability test. Proceedings of Japan Concrete Institute, 40(1) (2018) 1725-1730.

[49]- R.N. Uwazuruonye. Effects of pore void saturation degree on nondestructive tests for durability assessment of concrete structures. PhD Thesis. Yokohama National University, 2020. doi:10.18880 / 00013481.

[50]- R.N. Uwazuruonye, A. Hosoda, Investigation of the effects of saturation degree of permeable pore voids for appropriate covercrete quality evaluation by SWAT. Internet Journal of Society for Social Management Systems, 12(2) (2020) 87-97.

[51]- T. Ngoc, A. Hosoda, Y. Tsujita, A. Shirakawa, Mitigation of cracking in durable RC deck slab on multiple span steel box girder considering stepwise construction method and utilizing expansive additive. Proceedings in the Japan Concrete Institute, 43(1) 508-513.

[52]- A. Hosoda, T. Ibi, R. N. Uwazuruonye, Y. Daisuke. Investigation of the curing effect of tunnel lining concrete using a small-diameter balloon structure. in Japan Concrete Institute. (2021), 941-946.

[53]- R. JIS, 5210; Portland Cement. Japanese Standards Association: Tokyo, Japan, (2009).

[54]- R. JIS, 5211; Portland blast-furnace slag cement. Japanese Standards Association: Tokyo, Japan, (2009).

[55]- A. JIS, 6201; Fly ash for use in concrete. Japanese Standards Association: Tokyo, Japan, (2009).

[56]- R. Uwazuruonye, A. Hosoda. Degree of saturation of permeable pore space at covercrete and its effects on Surface Water Absorption Test (SWAT). in 73rd RILEM Week IMSCE Conference, Nanjing, China. (2019), 17.

[57]- C. Antón, M.A. Climent, G. de Vera, I. Sánchez, C. Andrade, An improved procedure for obtaining and maintaining well characterized partial water saturation states on concrete samples to be used for mass transport tests. Materials and Structures, 46(8) (2013) 1389-1400. doi:10.1617/s11527-012-9981-4.

Appendix A. Figure A shows the detailed geometry of the SWAT device while table A1 shows the conventional criterion for quality grading of covercrete.

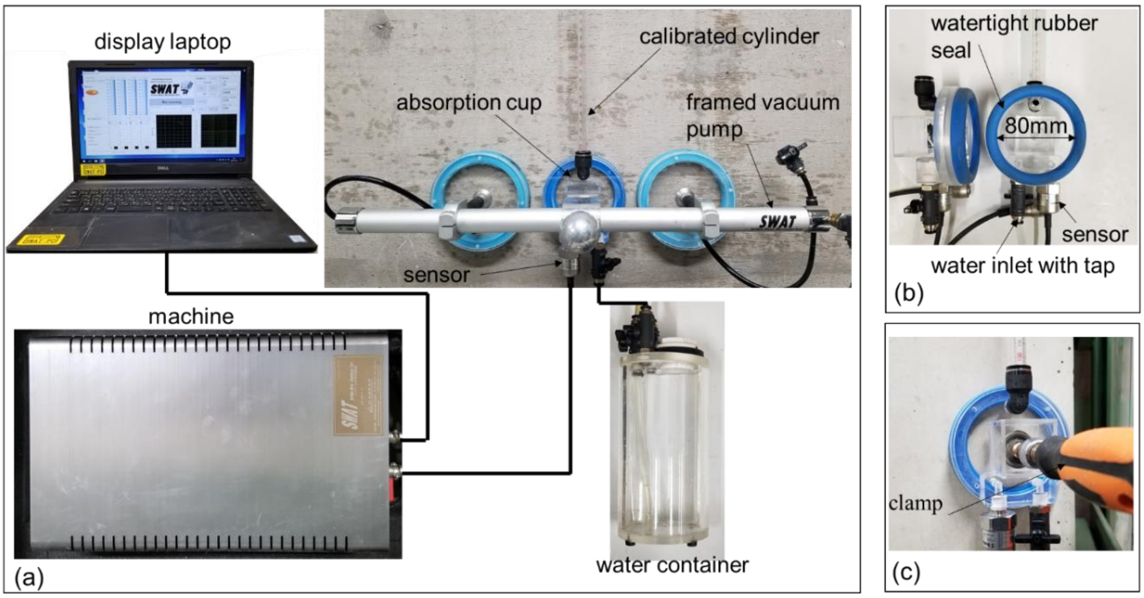

Fig. A – Detailed geometry of SWAT device (a) system (b) details of absorption cup (c) detail of attachment onto small specimen.

A.1. Covercrete quality grading table by SWAT

Index parameter	**Quality**		
	Good	Ordinary	Poor
p_{600} (ml/m^2/s)	< 0.25	0.25 – 0.50	> 0.50
CSWA (ml/m^2/s$^{1/2}$)	10 and below	11 – 20	> 20